Research Square

Preprints are preliminary reports that have not undergone peer review.
They should not be considered conclusive, used to inform clinical practice,
or referenced by the media as validated information.

Catalpol improves senile osteoporosis by promoting osteogenesis and inhibiting bone resorption through the PI3K/AKT signaling pathway

Zenghui Tian
Shandong University of Traditional Chinese Medicine
Kaiying Cui
Affiliated Hospital of Shandong University of Traditional Chinese Medicine
Yuxiao Tian
Shandong University of Traditional Chinese Medicine
Cunliang Guo
Affiliated Hospital of Shandong University of Traditional Chinese Medicine
Guoyan Liu
Affiliated Hospital of Shandong University of Traditional Chinese Medicine
Xiaoying Wang
Jinan Vocational College of nursing
Yanke Hao
Affiliated Hospital of Shandong University of Traditional Chinese Medicine
Yingying Li
2024100089@sdutcm.edu.cn

Affiliated Hospital of Shandong University of Traditional Chinese Medicine

Article

Keywords: Catalpol, Senile osteoporosis, PI3K/AKT signaling pathway, osteogenesis, bone resorption

Posted Date: August 14th, 2026

DOI: https://doi.org/10.21203/rs.3.rs-9974943/v1

License: This work is licensed under a Creative Commons Attribution 4.0 International License.
Read Full License

Additional Declarations: No competing interests reported.

Abstract

Senile osteoporosis (SOP) is core pathology is the imbalance between bone formation and bone resorption, which leads to reduced bone mass and increased bone fragility. Catalpol possesses various biological activities such as antioxidant and anti-inflammatory effects. However, the mechanism by which it improves SOP remains unclear. This study aims to clarify the mechanism of catalpol in improving SOP through the PI3K/AKT signaling pathway. 24 SPF-grade male SD rats were randomly divided into four groups: normal control group, model group, experimental group, and positive control group. Micro-CT, HE, TRAP staining, immunohistochemistry, ELISA, and Western blot were used to detect relevant indicators. The results showed that after catalpol intervention, the bone microstructure parameters of the rat femur, such as BMD and Tb.N were significantly increased, while Tb.Sp was decreased. The number of osteoblasts was increased, and the number of osteoclasts was decreased. In the serum, the level of the bone formation marker PINP was elevated, and the level of the bone resorption marker β-CTX was reduced. In the bone tissue, the expression of osteogenic marker proteins was upregulated, and the expression of osteoclastic marker proteins was downregulated. Meanwhile, the expression of PI3K protein and the ratio of P-AKT to AKT were significantly increased. The above results indicate that catalpol can bidirectionally regulate bone metabolism by activating the PI3K/AKT signaling pathway. It promotes bone formation, inhibits bone resorption, restores bone homeostasis, and improves SOP, thereby holding promise as a potential candidate drug for the clinical prevention and treatment of SOP.

1. Introduction

Osteoporosis (OP) is a metabolic bone disease characterized by reduced bone mass, destruction and deterioration of bone tissue and microstructure, and decreased bone density, leading to increased bone fragility (1). A critical factor in the development of OP is the imbalance between bone formation and bone resorption, which results in heightened bone resorption and diminished bone formation, ultimately causing significant bone loss (2). Senile osteoporosis (SOP) has emerged as a global health concern due to the aging population, with 10.2% of adults over 50 years of age affected by the condition, a figure projected to rise to 13.6% by 2030 (3). Advances in clinical research have revealed that anti-OP treatment is a prolonged process, and patients undergoing long-term therapy with anti-OP medications may experience adverse events such as jaw necrosis, atrial fibrillation, fever, and myalgia (4). Furthermore, individuals with OP impose economic burdens on themselves and society due to the extended duration of drug therapy and healthcare needs (5). Consequently, there is a pressing need to develop efficient, cost-effective, and safe pharmacological options for the treatment of SOP.

In recent years, with the demonstrated efficacy of traditional Chinese medicine (TCM) in treating OP and the deepening of clinical research, natural bioactive products have attracted increasing attention as alternatives to clinical drugs for the prevention and treatment of OP (6). Rehmannia glutinosa Libosch, a TCM herb, has held an important place in the thousand-year history of TCM. It possesses effects such as nourishing blood and yin, benefiting the marrow, and replenishing essence, making it an indispensable

component of many medical prescriptions used to treat OP (7, 8). Catalpol, the main active component of Rehmannia glutinosa Libosch, exhibits strong biological activities including antioxidation, anti-inflammation, and anti-apoptosis (9). Current studies have shown that catalpol exerts anti-OP effects by promoting osteogenic differentiation via the Wnt/β-catenin signaling pathway and inhibiting osteoclast differentiation through pathways such as RANKL/RANK (10). The phosphatidylinositol 3-kinase (PI3K)/protein kinase B (AKT) pathway is widely involved in physiological processes such as cell proliferation, differentiation, survival, and metabolism (11), and is one of the most important intracellular signal transduction pathways. This pathway is not only closely associated with the proliferation and differentiation of osteoblasts, osteoclasts, and bone marrow mesenchymal stem cells, but also participates in bone metabolism and bone remodeling (12). Multiple studies have indicated that activating the PI3K/AKT signaling pathway can promote osteogenic differentiation (13) and inhibit osteoclast differentiation (14). Therefore, the PI3K/AKT signaling pathway plays a critical role in regulating bone homeostasis. However, the mechanism by which catalpol promotes bone formation, inhibits bone resorption, restores bone homeostasis, and improves OP through activation of the PI3K/AKT signaling pathway remains unclear.

This study therefore aims to elucidate the therapeutic mechanism of catalpol in OP by investigating its effects on PI3K/AKT signaling, osteogenic/osteoclast markers, and bone microstructure in a SOP model (Fig. 1). The findings will provide a solid experimental basis for clinical SOP prevention and treatment, thereby advancing the application of TCM in this field.

2. Materials and Methods

2.1 Experimental Animals and Grouping

Twenty-four 12-week-old male Sprague-Dawley (SD) rats (weighing 240–300 g) were purchased from Shandong Pengyue Laboratory Animal Technology Co., Ltd. (license number: SCXK (Lu) 2022 0006). The rats were housed in an SPF-grade facility at the Animal Experiment Center of the Affiliated Hospital of Shandong University of Traditional Chinese Medicine. The housing environment was maintained at a temperature of 22–26°C, relative humidity of 50 ± 5%, and a 12-hour light/dark cycle, with food and water available ad libitum.

Using a random number table, the rats were randomly assigned to four groups (n = 6 per group): the normal control (NC) group, model (M) group, experimental (E) group, and positive control (PC) group. The experimental protocol was approved by the Laboratory Animal Ethics Committee of Shandong University of Traditional Chinese Medicine (approval number: SDSZYYAWE20250319001). All animal experiments were performed according to the ARRIVE guidelines.

2.2 Main Experimental Drugs, Reagents, and Instruments

Catalpol (Chengdu Must Bio-technology Co., Ltd);Alendronate Sodium Tablets (National Drug Approval Number: H20059029; Specification: 70 mg×4 tablets; Beijing Foyou Pharma Co., Ltd);D-Galactose

(Shanghai Macklin Biochemical Co., Ltd);Micro CT (Model: NC-200);Multicolor Fluorescence Imaging System (Model: GE Amersham Imager600);Embedding Machine (Model: JB-P5);Paraffin Microtome (Leica RM2255);Automatic Section Analysis System (Model: HS6);BCA Protein Quantification Kit (Catalog No.: P0010; Beyotime Biotech Inc);Hematoxylin-Eosin (HE) Staining Kit (Catalog No.: G1120; Beijing Solarbio Science & Technology Co., Ltd);Rat Procollagen I N-Terminal Propeptide (PINP) ELISA Kit (Catalog No.: JL13510; Shanghai Jonlnbio Industrial Co., Ltd);Rat Beta-Crosslaps (b-CTx) ELISA Kit (Catalog No.: JL51641; Shanghai Jonlnbio Industrial Co., Ltd);Anti-Osteocalcin Rabbit pAb (Catalog No.: GB11233; Wuhan Servicebio Technology Co., Ltd);Anti-MMP-9 (Catalog No.: 27306-1-AP; Proteintech);Anti-RANKL (Catalog No.: 23408-1-AP; Proteintech);Anti-RUNX2 (Catalog No.: 20700-1-AP; Proteintech);Anti-P65 (Catalog No.: 80979-1-RR; Proteintech);Anti-Osteopontin (Catalog No.: 22953-1-AP; Proteintech);Anti-Collagen (Catalog No.: 14695-1-AP; Proteintech); PI3 Kinase p110 Beta Polyclonal antibody (cat. no. 20584-1-AP, Proteintech Group, Inc) AKT Polyclonal antibody (cat. no. 10176-2-AP, Proteintech Group, Inc); Phospho-AKT (Ser473) Polyclonal antibody (cat. no. 28731-1-AP, Proteintech Group, Inc); Beta Actin Polyclonal antibody (cat. no. 20536-1-AP, Proteintech Group, Inc); Horseradish Peroxidase (HRP)-conjugated Goat Anti-Rabbit IgG (Catalog No.: 20536-1-AP; Proteintech).

2.3. Model Establishment, Drug Administration, and Experimental Procedures

After one week of acclimatization, the rats were subjected to the following treatments for 90 days:

NC-group: Intraperitoneal injection of 0.9% normal saline at 5 mL/kg/day, plus daily oral gavage of normal saline at 5 mL/kg.

M-group: Intraperitoneal injection of D-galactose at 100 mg/kg/day, plus daily oral gavage of normal saline at 5 mL/kg.

E-group: Intraperitoneal injection of D-galactose at 100 mg/kg/day, plus daily oral gavage of catalpol at 100 mg/kg.

PC-group: Intraperitoneal injection of D-galactose at 100 mg/kg/day, plus daily oral gavage of alendronate sodium at 1.428 mg/kg.

A significant decrease in bone mineral density (BMD) was observed in the M-group compared to the NC-group ($P < 0.05$), confirming the successful establishment of the OP model. During the experiment, the rats were weighed weekly. They were fasted overnight with free access to water before each weighing, which was performed prior to drug administration on the following day. Dosages for the subsequent week were adjusted based on the recorded body weight. Upon completion of the experiment, all rats were anesthetized via an intraperitoneal injection of 3% pentobarbital sodium (1.5 mL/kg). Blood samples were collected from the abdominal aorta, followed by euthanasia via cervical dislocation. The blood samples were allowed to clot, centrifuged at 3500 r/min at 4°C for 15 minutes, and the resulting supernatant (serum) was collected, aliquoted, and stored at -80°C for subsequent analysis of bone

metabolism indices. Bilateral femurs were harvested: the right femur was fixed in 4% paraformaldehyde for further analysis, and the left femur was stored at -80°C for future use.

2.4 Animal sacrifice

All rats were anesthetized by intraperitoneal injection of 3% pentobarbital sodium (1.5 mL/kg) and subsequently euthanized via cervical dislocation. The absence of vital signs was confirmed to verify successful death.

2.5. Experimental Assessments

2.5.1. General Health Status and Body Weight

The rats' diet, fur condition, and general activity status were observed weekly.

2.5.2. Femoral Micro-CT Analysis

The right femurs from rats in each group were collected and subjected to Micro-CT scanning. Following the scan, the original images were reconstructed three-dimensionally using the NRecon software. A standardized Region of Interest (ROI) was analyzed with CT Analyzer (version 1.20.3.0) to quantitatively assess the bone microstructure. The following parameters were calculated: BMD, Bone Volume/Tissue Volume (BV/TV), Trabecular Number (Tb.N), average Trabecular Thickness (Tb.Th(avg)), average Trabecular Separation (Tb.Sp(avg)), and Trabecular Connectivity Density (Conn.D).

2.5.3. Histological Staining of Femoral Tissue

The right femurs from each group were fixed in 4% paraformaldehyde for 24 hours and then submerged in a 15% EDTA decalcification solution. The decalcification solution was changed every three days until completion, which was confirmed by physical inspection. Following decalcification, the femurs were dehydrated, embedded in paraffin, and serially sectioned into 3.0–4.0 μm thick slices. The sections were stained with Hematoxylin and Eosin (H&E) according to the manufacturer's protocol. Histopathological changes in the trabecular bone, including its number and morphology, were observed under a microscope.

2.5.4. Immunohistochemical Analysis

Osteocalcin (OCN), a protein primarily secreted by osteoblasts, was detected to reflect osteoblast activity and bone formation (15). For immunohistochemistry, tissue sections were first subjected to antigen retrieval in EDTA buffer (pH 9.0). After washing three times with PBS, the sections were incubated overnight with a primary antibody diluted in PBS at a specified ratio. Subsequently, the slides were washed three times with PBS (pH 7.4) and incubated with a secondary antibody. Nuclei were counterstained with DAPI, and the sections were finally mounted. Images were captured under a microscope using consistent fields of view. For each section, three non-overlapping fields of identical dimensions were randomly selected, and the absorbance values were analyzed using ImageJ software.

2.5.5. artrate-Resistant Acid Phosphatase (TRAP) Staining

Osteoclast numbers were determined by TRAP staining to assess osteoclast activity in rat bone tissue. Following dewaxing and rehydration, the sections were incubated in TRAP staining buffer for 1 hour at 37°C, rinsed with distilled water, and counterstained with hematoxylin for 5 minutes. Finally, the sections were dehydrated, cleared, and mounted with gum. Sections from each group were imaged under a microscope using consistent fields of view. Three non-overlapping fields of identical dimensions were randomly selected at the same magnification for the observation of TRAP-positive osteoclasts.

2.5.6. Measurement of Serum PINP and β-CTX Levels by ELISA

Procollagen I N-terminal propeptide (PINP) and Beta-Crosslaps (β-CTX) are recommended by the International Osteoporosis Foundation (IOF) and the International Federation of Clinical Chemistry and Laboratory Medicine (IFCC) as bone turnover markers of high sensitivity (16). In this study, serum levels of PINP and β-CTX were determined using enzyme-linked immunosorbent assay (ELISA) to evaluate bone metabolism. All reagents and serum samples were brought to room temperature prior to the assay, which was performed according to the manufacturer's instructions. Briefly, the procedure included: coating the plate, adding standards and samples, adding detection antibodies, sealing and incubating the plate for 2 hours at room temperature, washing, adding enzyme conjugate and incubating for 45 minutes, washing again, adding chromogenic substrate, stopping the reaction, and finally measuring the absorbance with a microplate reader. The concentrations of PINP and β-CTX were calculated based on the standard curve.

2.5.7. Western Blot Analysis of Bone Tissue Proteins

The left femurs from rats in each group were pulverized in a mortar with repeated addition of liquid nitrogen. The resulting powder was homogenized in lysis buffer at 4°C using a homogenizer, with intermittent shaking every 5 minutes for a total of 8 cycles, followed by centrifugation for 15 minutes. The supernatant was collected, and total protein was extracted and quantified using the BCA method. The protein samples were denatured by boiling with loading buffer for 10 minutes. Subsequently, 20 μg of protein per sample was separated by SDS-PAGE and transferred onto a polyvinylidene fluoride (PVDF) membrane. The membrane was blocked with 5% skimmed milk at room temperature for 3 hours, incubated with primary antibodies at 4°C overnight, and then with horseradish peroxidase (HRP)-conjugated secondary antibodies at room temperature for 1 hour. After each antibody incubation, the membrane was washed thoroughly. Protein bands were visualized using an enhanced chemiluminescence (ECL) reagent. GAPDH was used as the internal control, and the band intensities were analyzed using ImageJ software. To conserve primary antibody consumption, polyvinylidene fluoride (PVDF) membranes were cut into strips prior to antibody incubation, and each strip was incubated with a specific primary antibody targeting the corresponding protein of interest. In accordance with the standard laboratory procedures, the intact uncut membranes were not imaged before cutting. All raw unprocessed images of individual membrane strips (containing complete membrane edges and molecular weight markers) have been provided in the supplementary file (Supplementary 1). All western

blot experiments were conducted in biological triplicate, and only representative immunoblot images are presented in the main figures.

2.6 Data Analysis

All data are presented as the mean ± standard deviation from three independent experiments. Statistical analyses were performed using SPSS 26.0 (IBM, USA). One-way analysis of variance (ANOVA) was conducted, followed by post hoc comparisons using either the Least Significant Difference (LSD) test or Dunnett's T3 test. A p-value of less than 0.05 was considered statistically significant. Graphs were generated using GraphPad Prism 6.0.

3. Results

3.1. Comparison of General Conditions Across Rat Groups

Rats in the NC-group exhibited dense, soft, and glossy fur, along with normal levels of food and water intake, mental alertness, and locomotor activity. In contrast, rats in the M-group developed loose, coarse, and dull fur that was prone to shedding. While their consumption and mental state remained normal, their locomotor activity was noticeably reduced. Compared to the M-group, both the E-group and PC group showed significant improvement in coat quality, presenting with shiny, dense, and soft fur, with no other marked differences in general condition. However, the fur quality of the PC-group appeared somewhat less glossy, looser, and coarser than that of the E-group, although no other significant differences were observed between these two groups.

3.2. Femoral Micro-CT Analysis in Rats

Three-dimensional reconstruction of the distal femur revealed a substantial reduction in trabecular number, impaired continuity, and widened trabecular separation in the M-group compared to the NC-group. In contrast, both the E- and PC-groups exhibited a marked increase in trabecular number, improved continuity, and reduced trabecular separation relative to the M-group. However, the PC-group showed relatively fewer trabeculae, poorer continuity, and larger trabecular gaps compared to the E-group (Fig. 2A).

Quantitative analysis of bone microstructure indicated that, compared to the NC-group, the M-group showed significantly lower values for BMD, BV/TV, Tb.N, Tb.Th, and Conn.D ($P < 0.05$), whereas Tb.Sp(avg) was significantly increased ($P < 0.05$). Relative to the M-group, both the E- and PC-groups demonstrated significant increases in BMD, BV/TV, Tb.N, Tb.Th(avg), and Conn.D ($P < 0.05$), along with a significant decrease in Tb.Sp(avg) ($P < 0.05$). Notably, the E-group displayed higher mean values for BMD, BV/TV, Tb.N, Tb.Th, and Conn.D, and lower trabecular separation than the PC-group (Fig. 2B-G).

3.3. Histopathological Assessment of Bone Tissue by H&E Staining

Compared with the NC-group, the M-group exhibited a significant reduction in trabecular number, thinning of trabeculae, widened and frequently fractured intertrabecular spaces, and a disrupted trabecular network. In contrast, both the E- and PC-groups showed increased trabecular number and thickness, improved continuity, and a partially restored trabecular network relative to the M-group. Notably, the E-group demonstrated markedly thicker trabeculae, whereas the PC-group primarily exhibited an increase in trabecular number and a relatively distinct network architecture (Fig. 3A).

3.4. Assessment of Osteoclast Activity in Rat Bone Tissue by TRAP Staining

TRAP staining revealed a significant increase in the number of TRAP-positive (red-stained) osteoclasts and an enlarged positive area in the M-group compared to the NC-group. In comparison to the M-group, both the E- and PC-groups showed a gradual reduction in the number of stained osteoclasts and a contraction of the positive area. The decrease in osteoclast number was more pronounced in the E-group than in the PC-group (Fig. 3B, D).

3.5. Immunohistochemical Evaluation of Osteoblast Activity and Bone Formation

Quantitative analysis demonstrated that the positive staining area in the M-group was significantly reduced compared to that in the NC-group ($P < 0.05$). Conversely, the positive areas in both the E- and PC-groups were increased relative to the M-group ($P < 0.05$). Among the treatment groups, the E-group presented a larger positive area than the PC-group (Fig. 3C, E).

3.6. Serum Levels of PINP and β-CTX in Rats

Compared with the NC-group, the M-group exhibited a significant decrease in the serum level of PINP ($P < 0.05$) and a significant increase in β-CTX ($P < 0.05$). Relative to the M-group, both the E- and PC-groups showed significantly increased serum PINP levels and decreased β-CTX levels ($P < 0.05$). Notably, the modulation of these serum biomarkers was markedly more pronounced in the E-group than in the PC-group (Fig. 3F, G).

3.7. Catalpol Promotes Osteogenesis and Inhibits Osteoclastogenesis

To further verify the role of catalpol in bone remodeling, we detected the expression of key proteins related to bone formation and resorption (Fig. 4A, B). Western blot analysis revealed that the expression of osteogenic proteins (COL1, RUNX2, and OPN) was significantly downregulated in the M-group compared to the NC-group ($P < 0.05$), indicating impaired bone formation. Conversely, the expression of osteoclast-related proteins (RANKL, MMP-9, and NF-κβ) was significantly upregulated ($P < 0.05$), suggesting enhanced bone resorption. Treatment with catalpol (E-group) significantly reversed these changes, increasing the levels of COL1, RUNX2, and OPN ($P < 0.05$) and decreasing the levels of RANKL, MMP-9, and NF-κβ ($P < 0.05$) compared to the M-group. Although the positive control (PC-group) showed

similar trends, the effects of catalpol were consistently more potent. These results demonstrate that catalpol ameliorates OP by coordinately promoting osteogenic activity and suppressing osteoclastogenesis (Fig. 4D-I).

3.8. Catalpol Activates the PI3K/AKT Signaling Pathway

To explore the mechanism by which catalpol improves bone metabolism, we examined the PI3K/AKT signaling pathway (Fig. 4C). The results showed that the protein expression of PI3K and the phosphorylation ratio of AKT (p-AKT/AKT) were significantly downregulated in the M-group compared to the NC-group ($P < 0.05$). In contrast, catalpol treatment (E-group) significantly upregulated both PI3K expression and AKT phosphorylation compared to the M-group ($P < 0.05$). Notably, the total AKT protein level remained unchanged across all groups ($P > 0.05$), indicating that the observed effects were specific to pathway activation rather than alterations in total protein abundance. The positive control (PC-group) showed a similar but less potent effect than the E-group (Fig. 4J-L). These findings indicate that catalpol activates the PI3K/AKT signaling pathway by upregulating PI3K expression and promoting AKT phosphorylation.

4. Discussion

The global population is aging at an accelerating rate, leading to a sharp increase in the prevalence of OP. Consequently, there is an urgent worldwide need to develop efficient, low-cost, and safe anti-osteoporotic drugs (17). Catalpol, an active component of traditional medicines used for OP, is known to modulate the functions of osteoblasts and osteoclasts. However, further investigation was required to confirm its therapeutic potential and mechanism of action in OP. Therefore, this study established a SOP rat model via D-galactose injection to preliminarily explore the interventional effects and underlying mechanisms of catalpol.

Micro-CT three-dimensional reconstruction revealed a significant reduction in trabecular bone number, poor continuity, and enlarged trabecular gaps in the M-group. In contrast, the E-group exhibited a significant increase in trabecular number, improved continuity, and reduced trabecular gaps. Quantitative analysis of bone microstructure demonstrated significant decreases in femoral BMD, BV/TV, Tb.N, Tb.Th, and Conn.D, alongside a significant increase in Tb.Sp in the M-group ($P < 0.05$). Conversely, the E-group showed significant increases in these parameters (except Tb.Sp, which decreased). Histopathological results were consistent, indicating thinner trabeculae with widened, frequently fractured gaps and a disrupted reticular structure in the M-group, all of which were ameliorated in the E-group, which exhibited thicker, more numerous trabeculae with improved continuity and a partially restored network. Notably, the outcomes in the E-group were superior to those in the positive control group. Collectively, these findings demonstrate that catalpol effectively improves bone quality.

Bone homeostasis is maintained through the balanced processes of osteoclast-mediated bone resorption and osteoblast-mediated bone formation, a crucial remodeling cycle for bone tissue renewal. The disruption of this balance leads to OP (18, 19). With aging, bone metabolism becomes dysregulated,

shifting towards a state of dominant bone resorption and negative bone remodeling balance, ultimately resulting in SOP. Therefore, a key therapeutic strategy for SOP is to promote bone formation, inhibit bone resorption, and restore metabolic equilibrium (20).

Osteoblasts are the primary cells responsible for the complex process of bone formation, which involves various osteogenic genes. OCN, a bone-derived hormone and indicator of bone turnover, reflects osteoblast activity and bone formation status (21). Immunohistochemical analysis showed a significantly increased OCN-positive area and a greater number of osteoblasts in the catalpol-treated (E) group compared to the M-group. PINP, a marker of collagen deposition, reflects the synthesis rate of the bone matrix and thus the level of bone formation (22). Our results showed a significant increase in serum PINP following catalpol intervention, indicating that catalpol accelerates bone formation by regulating bone matrix synthesis. RUNX is a key regulator of osteoblast differentiation and bone maintenance (23, 24). COL1, the main component of the extracellular matrix, is essential for bone matrix deposition and mineralization (25, 26). OPN, a multifunctional phosphoprotein in the bone matrix, is associated with bone turnover and remodeling (27). The detection of these osteogenic markers (RUNX2, COL1, OPN) reflects bone formation trends. Our experiments revealed decreased expression of these proteins in the M-group compared to the NC-group, which was reversed after catalpol intervention (E-group vs. M-group). In summary, catalpol promotes bone formation and ameliorates OP by increasing osteoblast numbers and enhancing their activity.

Osteoclastic resorption (bone resorption) is a metabolic process opposite to osteogenesis (bone formation). It is mainly manifested as a physiological behavior in which the volume and density of bone tissue gradually decrease under a relatively low stress level. The trend of bone resorption can be reflected by detecting osteoclast-related indicators (28). Tartrate-resistant acid phosphatase (TRAP) is an enzyme produced by osteoclasts; it is specifically distributed in and unique to osteoclasts, and is generally regarded as a crucial marker for identifying osteoclasts (29). By detecting the expression of TRAP, the number of osteoclasts in rat bone tissue and the status of bone resorption can be further evaluated. TRAP staining in our study showed a significantly reduced positive area and fewer osteoclasts in the E-group compared to the M-group. β-CTX a specific product of collagen degradation, reflects osteoclast activity and bone resorption (22). A significant decrease in serum β-CTX after catalpol intervention indicated suppressed osteoclast activity. Receptor Activator of Nuclear Factor-κB Ligand (RANKL) is a type II transmembrane protein belonging to the tumor necrosis factor (TNF) superfamily, and it serves as a key molecule linking the skeletal system and the immune system. Studies have shown (30) that when macrophage/dendritic cell progenitors are stimulated by RANKL, the initiation of the osteoclast differentiation process is triggered. Subsequently, multinucleated osteoclasts are formed through cell-cell fusion of pre-osteoclasts, preparing for bone resorption (31). Matrix metalloproteinases (MMPs) are a class of enzymes essential for bone remodeling, primarily responsible for the degradation of collagen (32). Studies have shown that MMP-9, the most abundant MMP in osteoclasts, acts as both a protease that activates genes encoding the master regulators of osteoclastogenesis and an epigenetic regulator that maintains osteoclast activation(33, 34). NF-κB (Nuclear Factor-kappa B) is a group of eukaryotic transcription factors that play a crucial role in various

pathophysiological processes. Meanwhile, NF-κB is also involved in multiple physiological processes such as cell growth, cell differentiation, and cell apoptosis. Studies have shown that the activation of NF-κB can promote the expression of specific genes in the osteoclast lineage to stimulate osteoclastogenesis (35). The expression of these osteoclast markers (RANKL, MMP-9, NF-κβ) reflects bone resorption trends. Our results demonstrated a significant increase in their expression in the M-group versus the NC-group, which was significantly suppressed after catalpol treatment (E-group vs. M-group). In conclusion, catalpol inhibits bone resorption and improves OP by reducing osteoclast numbers and suppressing their activity.

PI3K (Phosphoinositide 3-Kinase) is composed of a regulatory subunit (p85) and a catalytic subunit (p110). Its function is to phosphorylate phosphatidylinositol 4,5-bisphosphate (PIP2) into phosphatidylinositol 3,4,5-trisphosphate (PIP3) (36). AKT (Protein Kinase B) is a major downstream effector molecule of PI3K. Activated PI3K converts PIP2 into PIP3, and PIP3 then activates phosphoinositide-dependent kinase 1 (PDK1) and subsequently activates AKT. This constitutes one of the key pathways regulating cellular behaviors such as cell apoptosis, proliferation, and differentiation (37). The PI3K-AKT signaling pathway plays an important role in the physiological and pathological processes of osteoporosis (OP). In the context of osteoporosis, the dysregulation of the PI3K/AKT pathway exerts adverse effects on bone metabolism; however, effective improvement of osteoporosis can be achieved by promoting the activation of the PI3K-AKT signaling pathway (38, 39). Studies have shown that modulating the PI3K/AKT pathway promotes osteoblast proliferation and bone formation (40), while other evidence indicates it inhibits osteoclast differentiation (41). Notably, some reports demonstrate that activating this pathway can simultaneously inhibit bone resorption and promote osteogenic differentiation to counter estrogen deficiency-induced OP (42). Consistent with these findings, our study found decreased activity of the PI3K/AKT pathway in osteoporotic rats, which was significantly activated by catalpol treatment.

5. Conclusion

In summary, using a SOP rat model, this study employed Micro-CT, histopathology, bone metabolism markers, and signaling protein analysis to demonstrate that catalpol activates the PI3K/AKT signaling pathway. This activation facilitates a bidirectional regulation of bone metabolism, simultaneously promoting osteoblast-mediated bone formation and inhibiting osteoclast-mediated bone resorption, thereby restoring bone homeostasis and improving SOP. Our findings verify the mechanism of catalpol in treating SOP, identify a promising candidate drug for OP, and support the application of traditional Chinese medicine in managing SOP.

Abbreviations

SOP
senile osteoporosis
BMD

bone mineral density
Tb.N
trabecular number
Tb.Sp
trabecular separation
OP
osteoporosis
TCM
traditional Chinese medicine
PI3K
phosphatidylinositol 3-kinase
AKT
protein kinase B
NC
normal control
M
model
E
experimental
PC
positive control
HE
Hematoxylin-Eosin
PINP. Procollagen I N-Terminal Propeptide
β-CTX
Beta-Crosslaps
BV/TV
Bone Volume/Tissue Volume
Tb.N
Trabecular Thickness
Tb.Sp
Trabecular Separation
Conn.D
Connectivity Density
OCN
osteocalcin
TRAP
Tartrate-Resistant Acid Phosphatase
PINP
Procollagen I N-terminal propeptide

RANKL
Receptor Activator of Nuclear Factor-κB Ligand
TNF
tumor necrosis factor
MMPs
Matrix metalloproteinases.

Declarations

Funding information

This research was supported by 2024 Doctoral Quality Enhancement and Innovation Project, Shandong University of Traditional Chinese Medicine (YJSTZCX2024031); Shandong Provincial Medical and Health Science and Technology Project (202403100325).

Ethics declarations

The experimental protocol was approved by the Laboratory Animal Ethics Committee of Shandong University of Traditional Chinese Medicine (approval number: SDSZYYAWE20250319001), and the experiments were performed in accordance with the approved guidelines and regulations. The experiments complied with the ARRIVE guidelines.

Data availability

The raw data supporting the conclusion of this article will be made available by the authors, without undue reservation.

Declaration of competing interest

All authors declare that they have no known or potential competing financial interests or personal relationships that could have influenced the findings reported in this study.

Author Contributions

Z.T.; K.C.: Methodology, Software, Validation, Formal analysis, Data Curation, Writing - Original Draft, Visualization, prepared figures 1-4. Y.T.; C.G.: Software, Methodology, Data curation. G.L.; X.W.: Data curation. Y.L.; Y.H.: Conceptualization, Investigation. Methodology. All authors reviewed the manuscript.

References

1. Cao, Y. et al. Morinda Officinalis-derived extracellular vesicle-like particles: Anti-osteoporosis effect by regulating MAPK signaling pathway. *Phytomedicine: Int. J. phytotherapy phytopharmacology*. **129**, 155628 (2024).

2. Zhao, X. et al. Puerarin alleviates osteoporosis in rats by targeting the JAK2/STAT3 signaling pathway. *Biomolecules Biomed.* **24** (6), 1651–1661 (2024).
3. Harris, K., Zagar, C. A., Lawrence, K. V. & Osteoporosis Common Questions and Answers. *Am. Family Phys.* **107** (3), 238–246 (2023).
4. Ayers, C. et al. Effectiveness and Safety of Treatments to Prevent Fractures in People With Low Bone Mass or Primary Osteoporosis: A Living Systematic Review and Network Meta-analysis for the American College of Physicians. *Ann. Intern. Med.* **176** (2), 182–195 (2023).
5. Masurkar, P. P. & Rege, S. Marginal health care expenditures and health-related quality of life burden in patients with osteoporosis in the United States. *J. Am. Pharmacists Association: JAPhA*. **65** (2), 102315 (2025).
6. Hu, Y. et al. Oyster mantle-derived exosomes alleviate osteoporosis by regulating bone homeostasis. *Biomaterials* **311**, 122648 (2024).
7. Zhang, N. D. et al. Traditional Chinese medicine formulas for the treatment of osteoporosis: Implication for antiosteoporotic drug discovery. *J. Ethnopharmacol.* **189**, 61–80 (2016).
8. Tan, M., Li, Q., Yang, B., Wang, S. & Chen, Z. Insight of Chinese Herbal Medicine in Treating Osteoporosis: Achievements from 2013 to 2023. *Am. J. Chin. Med.* **52** (5), 1303–1328 (2024).
9. Zhang, Z., Dai, Y., Xiao, Y. & Liu, Q. Protective effects of catalpol on cardio-cerebrovascular diseases: A comprehensive review. *J. Pharm. Anal.* **13** (10), 1089–1101 (2023).
10. Li, N., Mu, X., Zhang, S. & Wang, H. Recent advances in the multifaceted mechanisms of catalpol in treating osteoporosis. *Front. Pharmacol.* **16**, 1560715 (2025).
11. Huang, H. et al. Rehmannioside A promotes the osteoblastic differentiation of MC3T3-E1 cells via the PI3K/AKT signaling pathway and inhibits glucocorticoid-induced bone loss in vivo. *J. Pharmacol. Sci.* **156** (4), 247–257 (2024).
12. Liu, C. et al. Research on the role and mechanism of the PI3K/Akt/mTOR signalling pathway in osteoporosis. *Front. Endocrinol.* **16**, 1541714 (2025).
13. Xin, L. et al. Exploring the osteogenic effects of simiao wan through activation of the PI3K/AKT pathway in osteoblasts. *J. Ethnopharmacol.* **338** (Pt 1), 119023 (2025).
14. Tang, K. et al. Neoandrographolide inhibits mature osteoclast differentiation to alleviate bone loss and treat osteoporosis. *Front. Pharmacol.* **16**, 1466057 (2025).
15. Taib, I. S. & Jayusman, P. A. The Role of Bone-Derived Osteocalcin in Testicular Steroidogenesis: Contributing Factor to Male Fertility. *Dis. (Basel Switzerland)* ;**12**(12). (2024).
16. Bhattoa, H. P. et al. Update on the role of bone turnover markers in the diagnosis and management of osteoporosis: a consensus paper from The European Society for Clinical and Economic Aspects of Osteoporosis, Osteoarthritis and Musculoskeletal Diseases (ESCEO), International Osteoporosis Foundation (IOF), and International Federation of Clinical Chemistry and Laboratory Medicine (IFCC). Osteoporosis international: a journal established as result of cooperation between the European Foundation for Osteoporosis and the National Osteoporosis Foundation of the USA. ;36(4):579–608. (2025).

17. Ma, S. et al. Zhuangyao Jianshen Wan ameliorates senile osteoporosis in SAMP6 mice through Modulation of the GCN5L1-mediated PI3K/Akt/wnt signaling pathway. *J. Orthop. translation*. **49**, 308–324 (2024).
18. Wu, Y. et al. Extracellular derivatives for bone metabolism. *J. Adv. Res.* **66**, 329–347 (2024).
19. Lee, S. J., Jang, S. A., Kim, S. C., Ryuk, J. A. & Ha, H. Lophatherum gracile Bronghiart Suppresses Receptor Activator of Nuclear Factor Kappa-B Ligand-Stimulated Osteoclastogenesis and Prevents Ovariectomy-Induced Osteoporosis. *Int. J. Mol. Sci.* ;**23**(22). (2022).
20. Bouvard, B. & Mabilleau, G. Gut hormones and bone homeostasis: potential therapeutic implications. *Nat. reviews Endocrinol.* **20** (9), 553–564 (2024).
21. Kang, N. et al. The role of osteocalcin in regulating the acute stress response. *Front. Pharmacol.* **16**, 1646558 (2025).
22. Chen, Y., Bai, R., Chen, W., Li, S. & Jiang, Y. Zhuang-Gu-Fang Treats Osteoporosis in Ovariectomized Rats by Increasing the Osteogenesis-Related Factors Leptin, Ghrelin, and PYY. Evidence-based complementary and alternative medicine. *eCAM* **2020**, 8164064 (2020).
23. Yalaev, B., Tyurin, A., Akhiiarova, K. & Khusainova, R. Hypomethylation of the RUNX2 Gene Is a New Potential Biomarker of Primary Osteoporosis in Men and Women. *Int. J. Mol. Sci.* ;**25**(13). (2024).
24. Akhiiarova, K., Khusainova, R., Minniakhmetov, I., Mokrysheva, N. & Tyurin, A. *Peak Bone Mass. Formation: Mod. View Problem Biomedicines* ;**11**(11). (2023).
25. Manochantr, S. et al. Improvement of osteogenic differentiation potential of placenta-derived mesenchymal stem cells by metformin via AMPK pathway activation. *Stem Cell Res. Ther.* **15** (1), 417 (2024).
26. Chen, Y. et al. Type-I collagen produced by distinct fibroblast lineages reveals specific function during embryogenesis and Osteogenesis Imperfecta. *Nat. Commun.* **12** (1), 7199 (2021).
27. Bai, R. J., Li, Y. S. & Zhang, F. J. Osteopontin, a bridge links osteoarthritis and osteoporosis. *Front. Endocrinol.* **13**, 1012508 (2022).
28. Wu, B. et al. A Novel Role for RILP in Regulating Osteoclastogenesis and Bone Resorption. Laboratory investigation; a journal of technical methods and pathology. ;103(5):100067. (2023).
29. Schini, M., Vilaca, T., Gossiel, F., Salam, S. & Eastell, R. Bone Turnover Markers: Basic Biology to Clinical Applications. *Endocr. Rev.* **44** (3), 417–473 (2023).
30. Zaidi, M. Skeletal remodeling in health and disease. *Nat. Med.* **13** (7), 791–801 (2007).
31. Honma, M., Ikebuchi, Y. & Suzuki, H. RANKL as a key figure in bridging between the bone and immune system: Its physiological functions and potential as a pharmacological target. *Pharmacol. Ther.* **218**, 107682 (2021).
32. Mustafa, F. E. A. et al. MMP-9 Expression in bone cells in the developing femur. *Tissue cell.* **95**, 102862 (2025).
33. Chen, Y. et al. Matrix Metalloproteinase-9 Enhances Osteoclastogenesis: Insights from Transgenic Rabbit Bone Marrow Models and In Vitro Studies. *Int. J. Mol. Sci.* ;**26**(7). (2025).

34. Shin, Y. et al. DNMT and HDAC inhibitors modulate MMP-9-dependent H3 N-terminal tail proteolysis and osteoclastogenesis. *Epigenetics chromatin*. **12** (1), 25 (2019).
35. Xue, C. et al. Aconine attenuates osteoclast-mediated bone resorption and ferroptosis to improve osteoporosis via inhibiting NF-κB signaling. *Front. Endocrinol.* **14**, 1234563 (2023).
36. Chen, P. H., Yao, H. & Huang, L. J. Cytokine Receptor Endocytosis: New Kinase Activity-Dependent and -Independent Roles of PI3K. *Front. Endocrinol.* **8**, 78 (2017).
37. Dong, J., Xu, X., Zhang, Q., Yuan, Z. & Tan, B. The PI3K/AKT pathway promotes fracture healing through its crosstalk with Wnt/β-catenin. *Exp. Cell Res.* **394** (1), 112137 (2020).
38. Guo, Y., Shen, K., Li, Z., Niu, C. & Luo, Y. MiR-147b-3p promotes osteogenesis by targeting NDUFA4 and PI3K/AKT pathway. *J. Orthop. Surg, Res.* **20** (1), 235 (2025).
39. Yin, R. et al. miR-140-3p aggregates osteoporosis by targeting PTEN and activating PTEN/PI3K/AKT signaling pathway. *Hum. Cell*. **33** (3), 569–581 (2020).
40. Liang, X. et al. Geraniin Promotes Osteoblast Proliferation, Bone Formation, and Autophagy by Regulating the PI3K/Akt/mTOR Cascade to Improve Glucocorticoid-Induced Osteoporosis. *Calcif. Tissue Int.* **116** (1), 77 (2025).
41. Han, J. et al. Eucommia, Cuscuta, and Drynaria Extracts Ameliorate Glucocorticoid-Induced Osteoporosis by Inhibiting Osteoclastogenesis Through PI3K/Akt Pathway. *Front. Pharmacol.* **12**, 772944 (2021).
42. Tan, C., Cong, S., Xie, Y. & Zhi, Y. Mechanistic Integration of Network Pharmacology and In Vivo Validation: TFRD Combat Osteoporosis via PI3K/AKT Pathway Activation. *Int. J. Mol. Sci.* ;**26**(8). (2025).

Figures

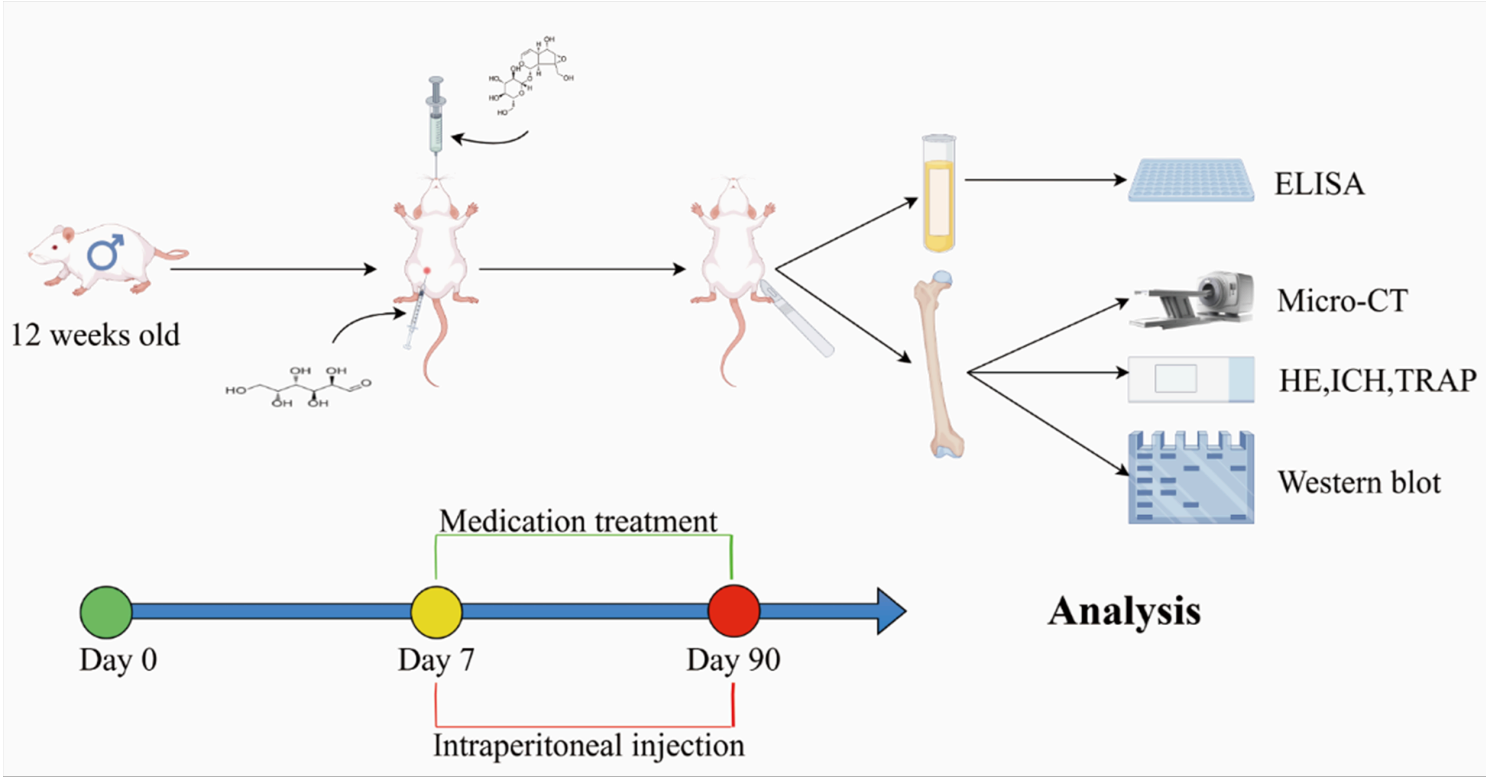


Figure 1

Flowchart of the animal experimental design.

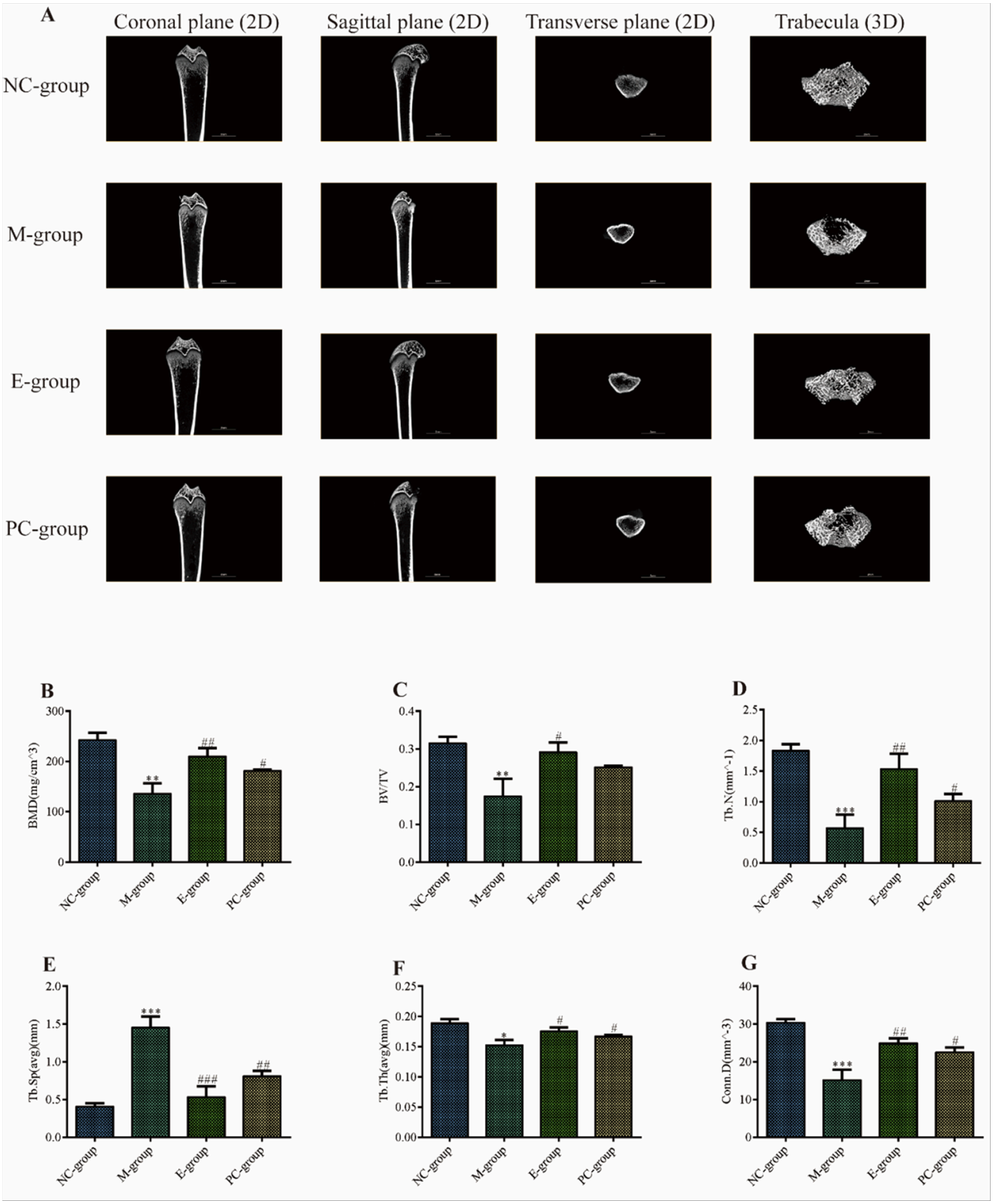


Figure 2

Effects of catalpol on bone microstructure in aged osteoporotic rats. (A) Representative micro-CT scanning and three-dimensional reconstruction images of rat femurs. (B-G) Quantitative analysis of bone microstructure parameters, including Bone Mineral Density (BMD), Bone Volume/Tissue Volume (BV/TV), Trabecular Number (Tb.N), Trabecular Thickness (Tb.Th), and Trabecular Connectivity Density

(Conn.D). Data are presented as mean ± SD. *P < 0.05, **P < 0.01, ***P < 0.001 vs. NC group; #P < 0.05, ##P < 0.01, ###P < 0.001 vs. M group.

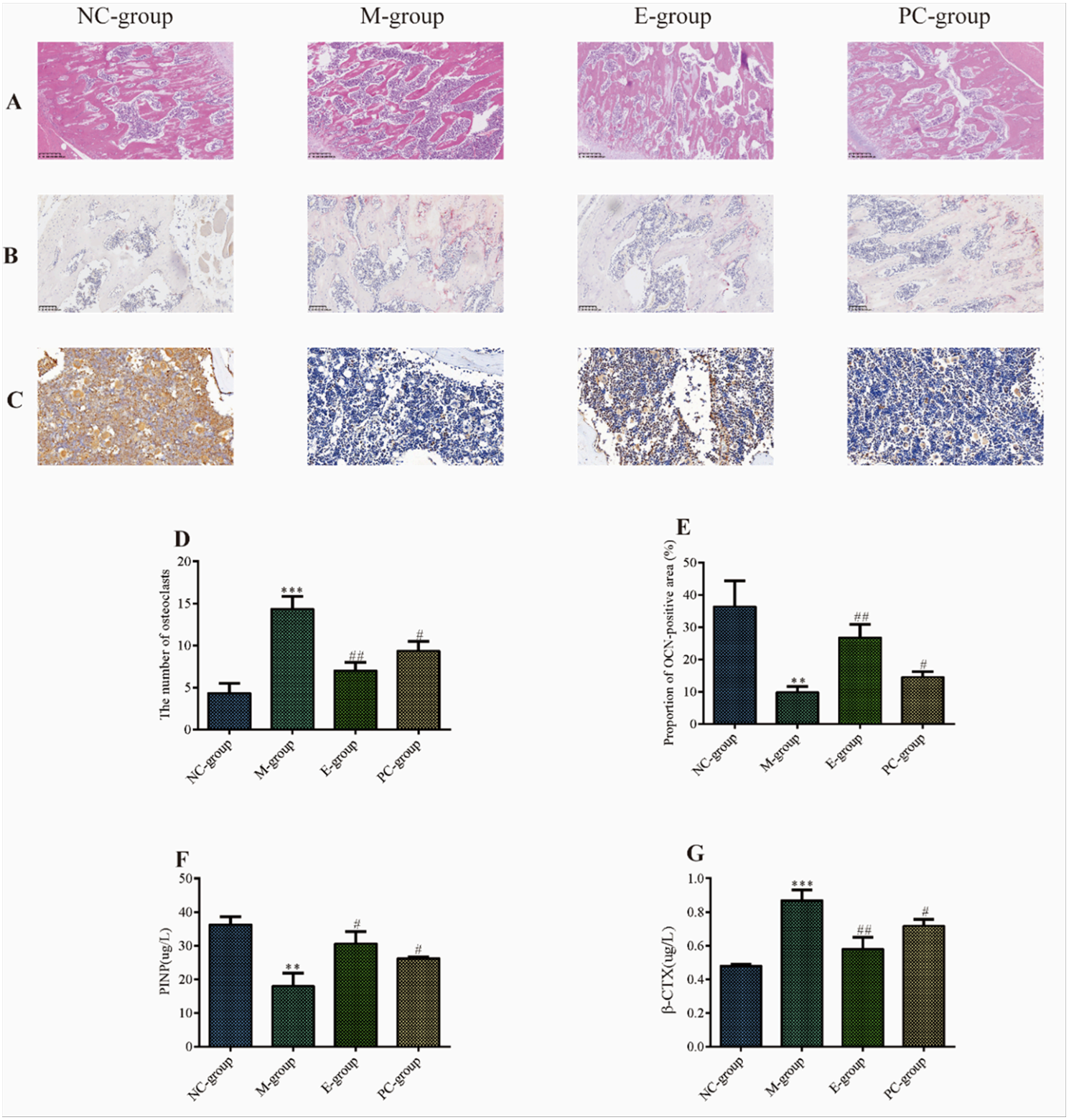


Figure 3

Effects of catalpol on bone histopathology, osteoclast activity, osteoblast activity, and serum bone metabolic markers. (A) Histological evaluation of femoral sections by hematoxylin and eosin (H&E)

staining. (B) Representative images of osteoclasts detected by tartrate-resistant acid phosphatase (TRAP) staining. (C) Representative immunohistochemical (IHC) images showing osteocalcin (OCN) expression in osteoblasts. (D) Quantitative analysis of osteoclast numbers from TRAP staining. (E) Quantitative analysis of OCN-positive area from IHC. (F, G) Serum levels of bone formation marker PINP and bone resorption marker β-CTX, as determined by ELISA. For all quantitative data (d-g), values are expressed as mean ± SD. *P < 0.05, **P < 0.01, ***P < 0.001 vs. NC group; #P < 0.05, ##P < 0.01, ###P < 0.001 vs. M group.

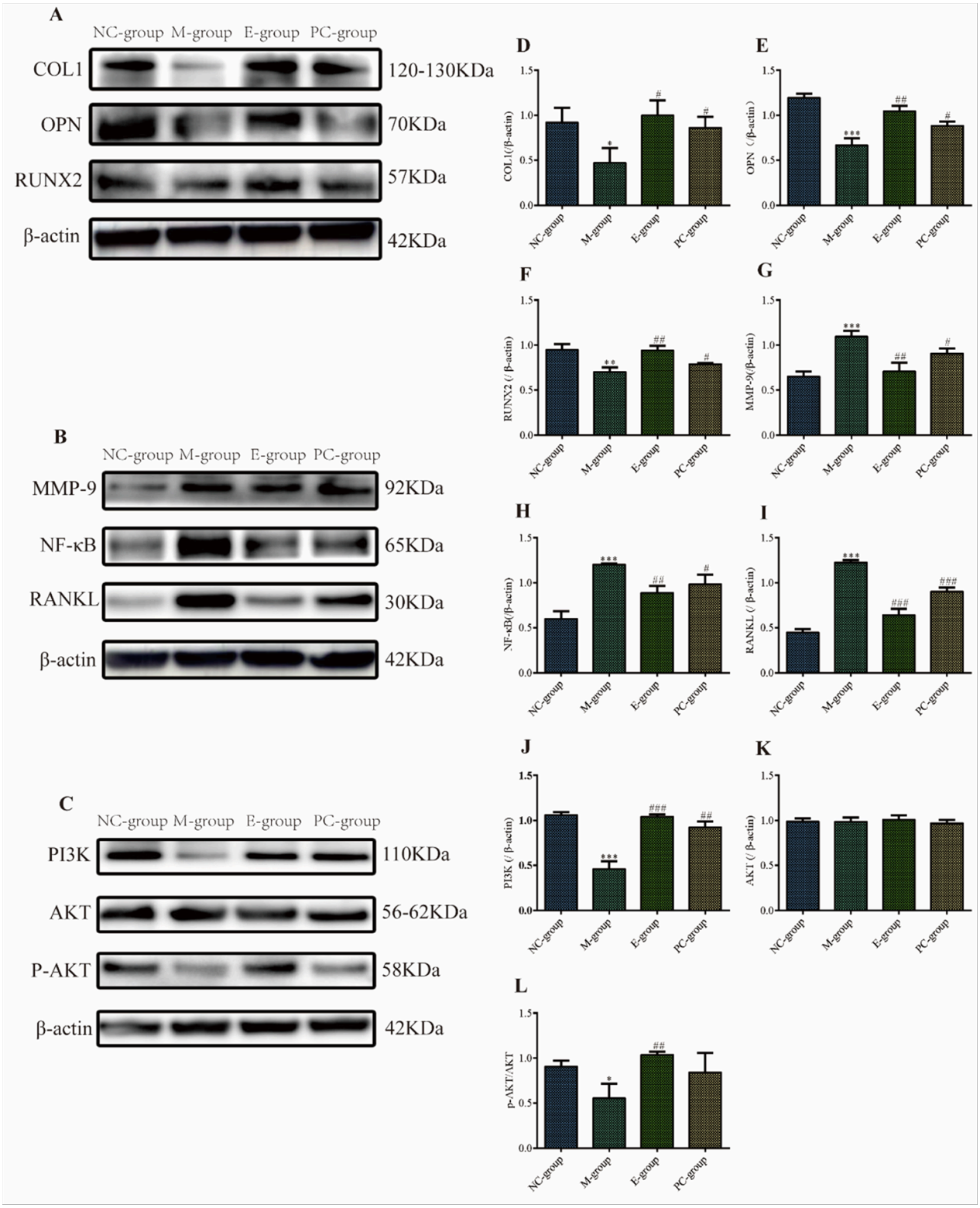


Figure 4

Effects of catalpol on the protein expression of osteogenic markers, osteoclastic markers, and key components of the PI3K/AKT pathway in bone tissue. (A-C) Representative Western blot bands showing the expression levels of. The original blots are presented in Supplementary 1. (A) osteogenic marker proteins (COL1, RUNX2, OPN), (B) osteoclastic marker proteins (RANKL, MMP-9, NF-κB), and (C) PI3K/AKT pathway proteins (PI3K, AKT, p-AKT). (D-L) Densitometric quantification of the protein levels shown in panels (A-C). Data are presented as mean ± SD. *P < 0.05, **P < 0.01, ***P< 0.001 vs. NC group; #P < 0.05, ##P < 0.01, ###P< 0.001 vs. M group.

Supplementary Files

This is a list of supplementary files associated with this preprint. Click to download.

- Supplementary1.pdf
- Supplementary1.zip